Numerical and analytical studies of critical radius in Cartesian and spherical geometries for corona discharge in air and CO_2-rich environments

Jacob A. Engle, Jeremy A. Riousset
Department of Physical Sciences, Center for Space and Atmospheric Research (CSAR), Embry-Riddle Aeronautical University, Daytona Beach, FL
(englej2@my.erau.edu)

Abstract

In order to determine the most effective geometry of a lightning rod, one must first understand the physical difference between their current designs. Benjamin Franklin's original theory of sharp tipped rods suggests an increase of local electric field, while Moore et al.'s (2000) studies of rounded tips evince an increased probability of strike (Moore et al., 2000; Gibson et al., 2009). In this analysis, the plasma discharge is produced between two electrodes with a high potential difference, resulting in ionization of the neutral gas particle. This process, when done at low current and low temperature can create a corona discharges, which can be observed as a luminescent emission. The Cartesian geometry known as Paschen, or Townsend, theory is particularly well suited to model experimental laboratory scenario, however, it is limited in its applicability to lightning rods. Franklin's sharp tip and Moore et al.'s (2000) rounded tip fundamentally differ in the radius of curvature of the upper end of the rod. As a first approximation, the rod can be modelled as an equipotential conducting sphere above the ground. Hence, we expand the classic Cartesian geometry into spherical and cylindrical geometries. In this work we explore the effects of shifting from the classical parallel plate analysis to spherical and cylindrical geometries more adapted for studies of lightning rods or power lines. Utilizing Townsend's equation for corona discharge, we estimate a critical radius and minimum breakdown voltage that allows ionization of the air around an electrode. Additionally, we explore the influence of the gas in which the discharge develops. We use BOLSIG+, a numerical solver for the Boltzmann equation, to calculate Townsend coefficients for CO2-rich atmospheric conditions (Hagelaar and Pitchford, 2005). This allows us to expand the scope of this study to other planetary bodies such as Mars. We solve the problem both numerically and analytically to present simplified formulas per each geometry and gas mixture. The development of a numerical framework will ultimately let us test the influence of additional parameters such as background ionization, initiation criterion, and charge conservation on the values of the critical radius and minimum breakdown voltage.

I. Introduction

Figure 1: Glow Coronas form on the edges of a powerline transformer (Berkoff, 2005).

Corona Discharge

- Electrical discharge around a conductor due to electric field;
- Weakly ionized gas responsible for glow at visible wavelengths;
- Hypothesized to promote the formation of upward connecting leaders in lightning discharges.

Electron Avalanche

The process of electron avalanching is similar between various types of discharges:

- Initial step of a discharge;
- Release of secondary electrons in electron-neutral collision;
- Secondary electrons with enough KE to repeat the process;
- Avalanche criteria:

$\int_{R_1}^{R_2} \alpha_{\text{eff}}\, dr = \ln(Q) \approx 18\text{-}20;\ Q = 10^4$

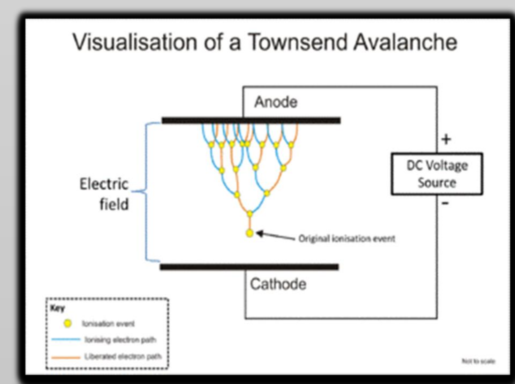

Figure 2: Visual representation of the process of an electron avalanche in Townsend's breakdown model. This can also be referred to as a Cartesian case due to the parallel plate structure (Gewartowski et al., 1965).

Types of Discharges

Parameter	Glow Corona	Streamer	Leader
Temperature	~300 K	~300 K	≳5000 K
Electron energy	1-2 eV	5-15 eV	1-2 eV
Electric field	0.2-2.7 kV/cm	5-7.5 kV/cm	1-5 kV/cm
Electron density	2.6×10^{8} cm^{-3}	5×10^{13}-10^{15} cm^{-3}	4×10^{14} cm^{-3}

Table 1: Characteristics for types of discharge at sea level [Adapted from (Gibson et al, 2009)].

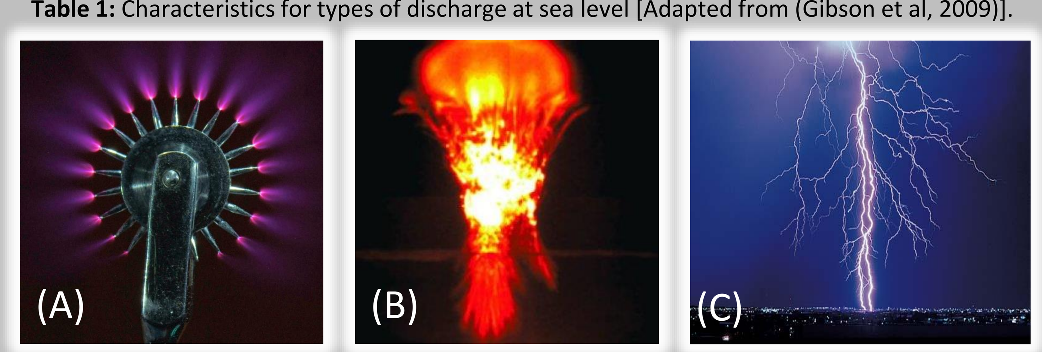

Figure 3: (A) A Wartenberg wheel in which glow Coronas form at the tip of each spindle. (Berkoff, 2005); (B) Streamers are the origin of a sprite phenomenon (courtesy of H. H. C. Stenbaek-Nielsen); (C) A lightning strike is perhaps the most common example of a leader discharge. (Whetmore, 2016).

Application to Martian Studies

Motivations:

- Potential hazard due to arcing on landers and rovers;
- Interfere with sensitive external systems and data measurements;
- Possible electrical shortage and failure.

Earth Analogy:

- Tribocharging in Martian dust storms akin to Earth sandstorms;
- Charge separation due to sedimentation & gravitation;
- Integration in the Martian global electric circuit.

Figure 4: (A) A dust storm on earth. The ionization behind this event could potentially create breakdown. (B) A dust storm photographed on the surface of Mars. The similarities between these two phenomenon indicate the possibility of breakdown potential on the surface of Mars. (C) The same dust storm on the surface of Mars seen from above. From (Yair, 2012).

Objectives

- Apply Paschen theory to Cartesian and spherical geometries;
- Obtain analytical expressions for critical radius and Stoletov's point;
- Develop numerical models for Cartesian and spherical geometries;
- Verify numerical models and analytical solutions with experimental data;
- Generalize to any atmosphere using a Boltzmann solver (Hagelaar and Pitchford, 2005);
- Establish the differences between sharp and blunt tipped rods for corona discharges in air and CO_2–rich atmospheres;

Assumptions

- $p = Nk_BT$
- $E(R_1) = E(c) = E_c \approx 30\,\frac{N_0}{N}\ kV/cm$ (Earth)
- $\nabla.\boldsymbol{E} = \rho_0 = 0$

II. Model Formulation

Geometry	Analytical Solution	Numerical Solution
Cartesian	• $\int_{x_1}^{x_2} \alpha_{\text{eff}} dx = \ln(Q)$ • $x_1 = 0$ • $\alpha_{\text{eff}}(E) = Ape^{\left(\frac{-Bp}{E}\right)}$ • $d = x_2 - x_1$ • $\frac{\partial V}{\partial d} = 0$: Stoletov's point	• $\int_{x_1}^{x_2} \alpha_{\text{eff}} dx = \ln(Q)$ • $x_1 = 0$ • $\alpha_{\text{eff}}(E) = \frac{\nu_i(E)-\nu_a(E)}{\mu_e(E)E}$ • $d = x_2 - x_1$ • $\frac{\partial V}{\partial d} = 0$: Stoletov's point • Boltzmann equation solver
Spherical	• $\int_{R_1}^{R_2} \alpha_{\text{eff}} dr = \ln(Q)$ • $R_2 \rightarrow \infty$ • $\alpha_{\text{eff}}(E) = Ape^{\left(\frac{-Bp}{E}\right)}$ • $\frac{\partial V}{\partial R_1} = 0$: Stoletov's point • $E(R_1) = E_c \frac{c^2}{{R_1}^2}$	• $\int_{R1}^{R2} \alpha_{\text{eff}} dr = \ln(Q)$ • $R_2 \rightarrow \infty$ • $\alpha_{\text{eff}}(E) = \frac{\nu_i(E)-\nu_a(E)}{\mu_e(E)E}$ • $\frac{\partial V}{\partial R_1} = 0$: Stoletov's point • Boltzmann equation solver • $E(R_1) = E_c \frac{c^2}{{R_1}^2}$

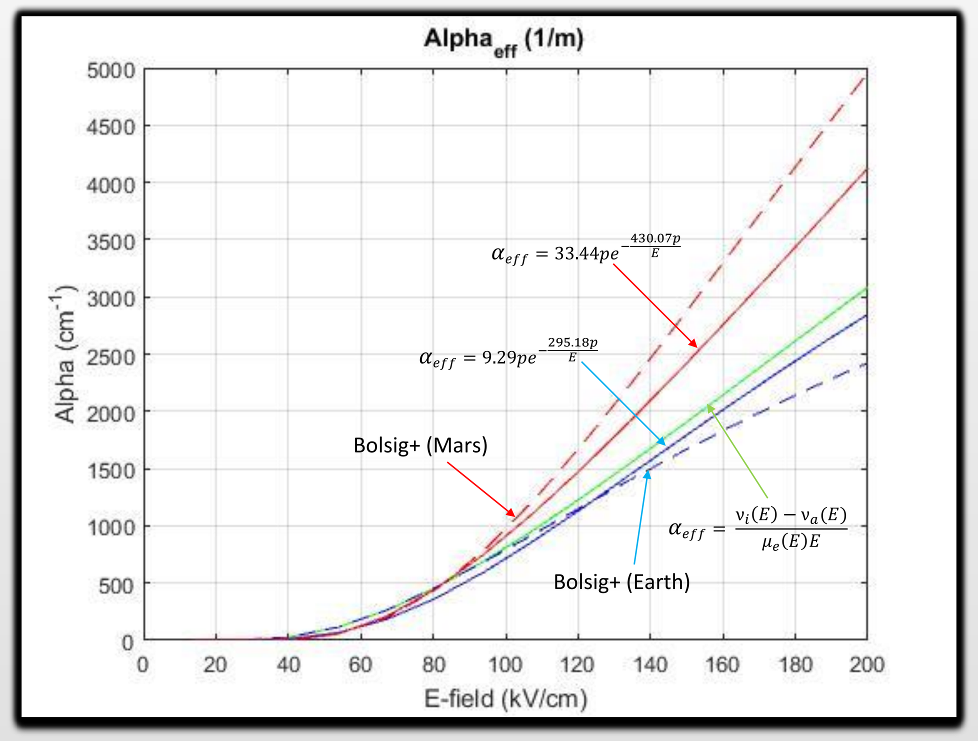

Figure 5: The exponential fit model of the exponential approximation for $\alpha_{\text{eff}}(E)$ for coefficients given by: Morrow and Lowke (1997), Hagelaar and Pitchford (2005).

III. Results and Discussion

Earth

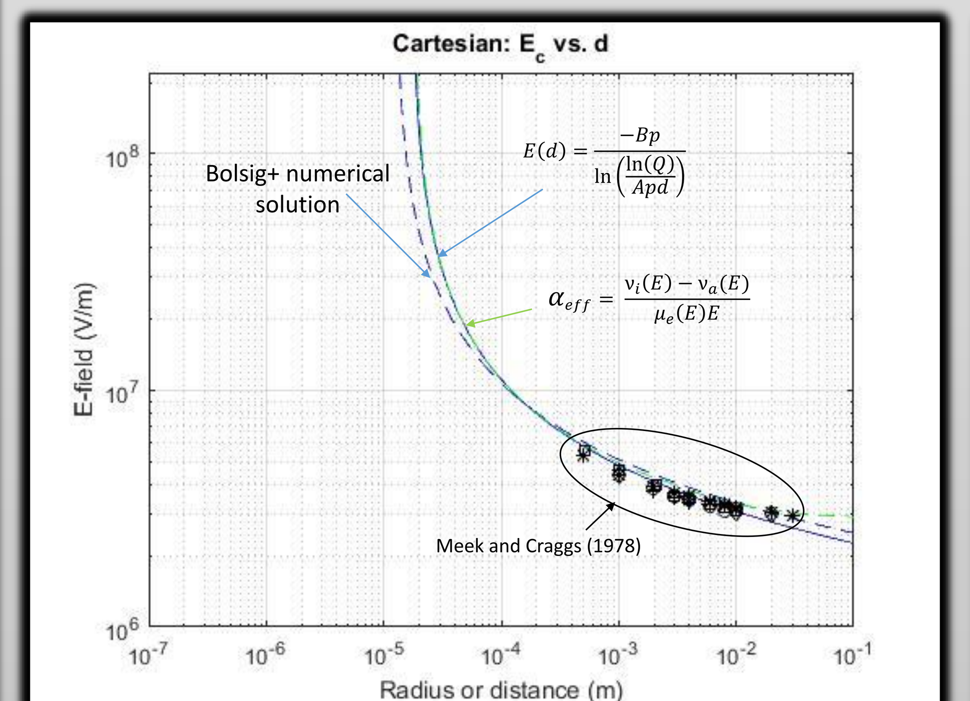

Figure 6: Analytical solution for electric field (E vs. d) as a function of d in Cartesian geometry $E(d) = \frac{-Bp}{\ln\left(\frac{\ln(Q)}{Apd}\right)}$

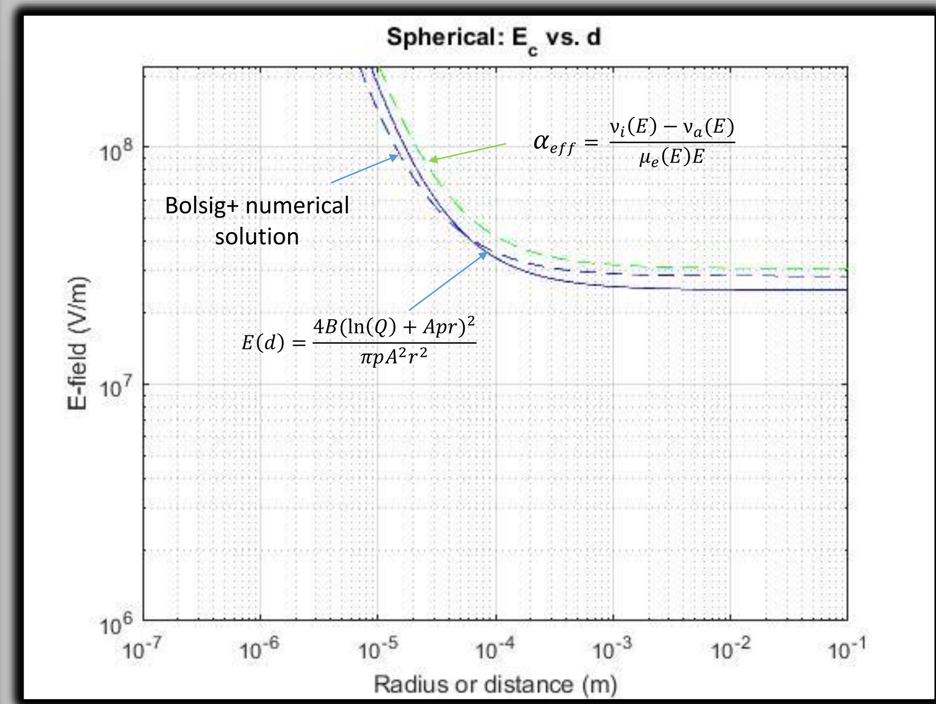

Figure 7: Analytical solution for electric field (E vs. d) as a function of r in Spherical geometry $E(r) = \frac{4B(\ln(Q)+Apr)^2}{\pi pA^2r^2}$

Mars

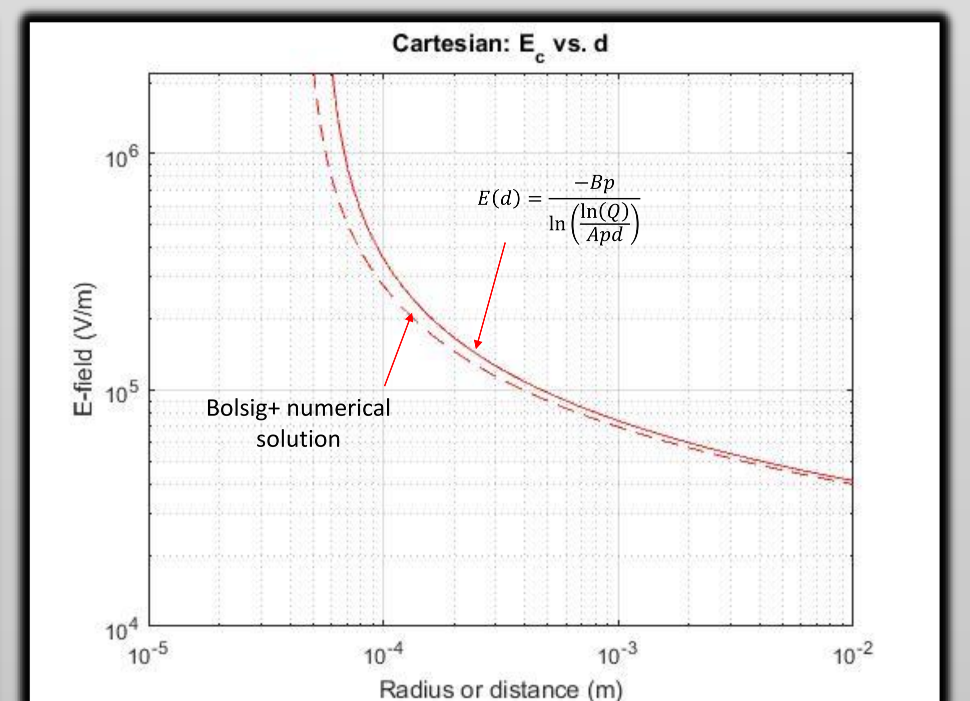

Figure 8: Analytical solution for electric field (E vs. d) as a function of d in Cartesian geometry $E(d) = \frac{-Bp}{\ln\left(\frac{\ln(Q)}{Apd}\right)}$

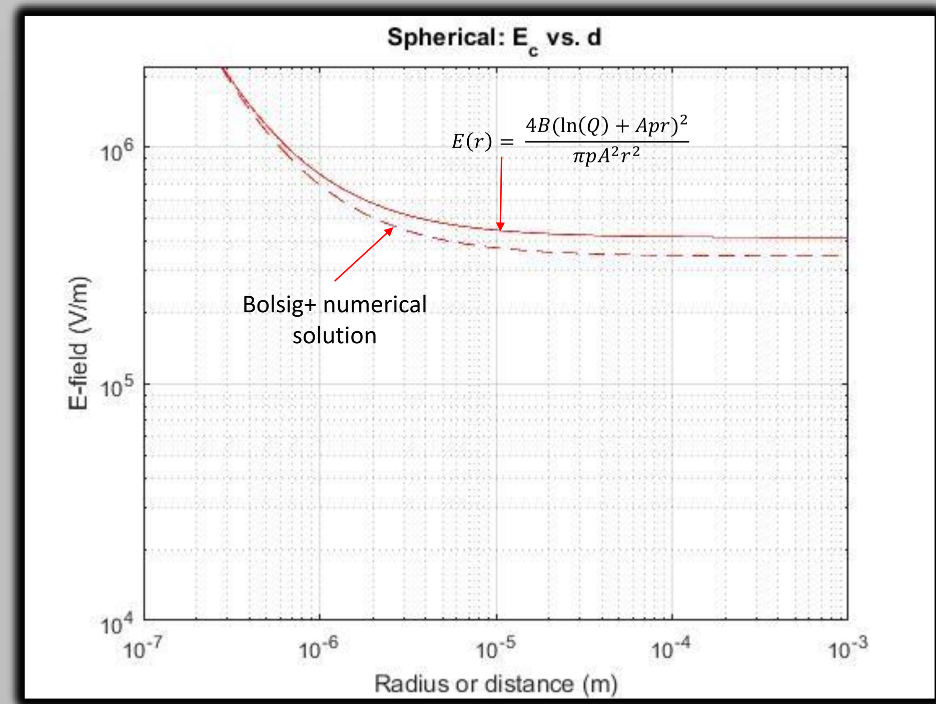

Figure 9: Analytical solution for electric field (E vs. d) as a function of r in Spherical geometry $E(r) = \frac{4B(\ln(Q)+Apr)^2}{\pi pA^2r^2}$

Paschen curves

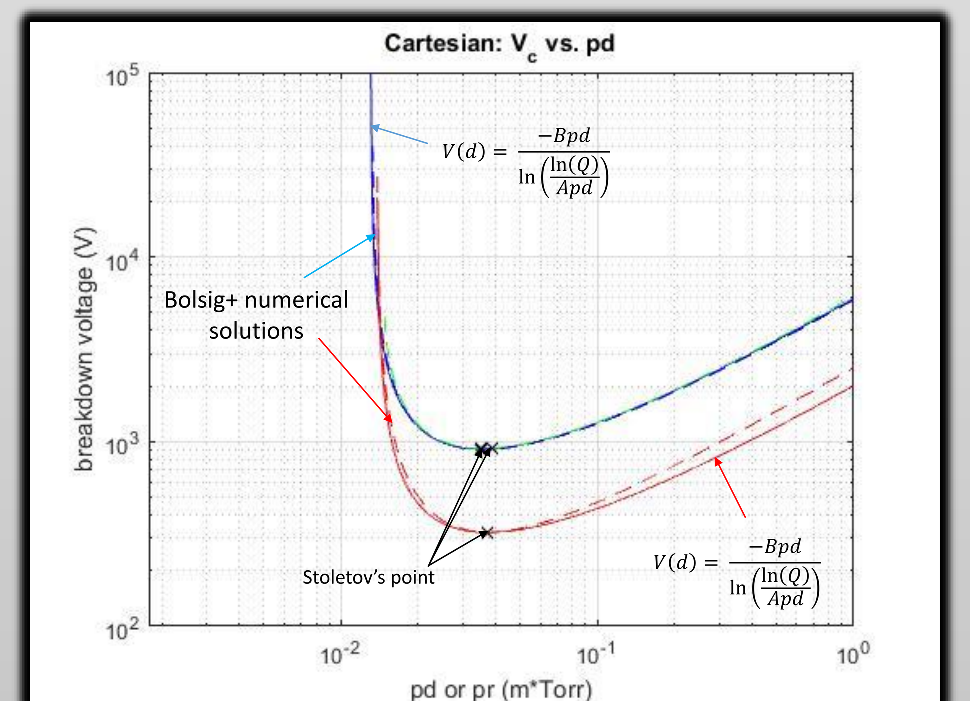

Figure 10: Paschen curves for Cartesian geometry

- Analytical solution $V(d) = \frac{-Bpd}{\ln\left(\frac{\ln(Q)}{Apd}\right)}$
- Stoletov's point $V_{min} = \frac{eB}{A}\ln(Q)$

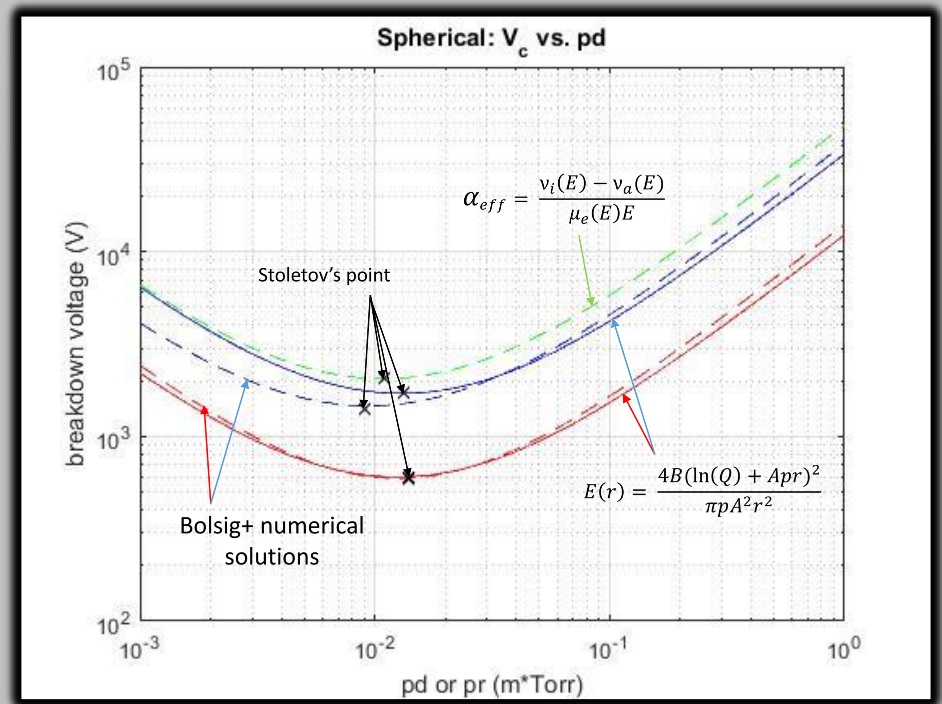

Figure 11: Paschen curves for spherical geometry

- Analytical solution $V(r) = \frac{4B(\ln(Q)+Apr)^2}{\pi pA}\left(\frac{1}{r_1} - \frac{1}{r_2}\right)$
- Stoletov's point $V_{min} = \frac{16B}{\pi A}\ln(Q)$

Coefficients and Stoletov's points

- A and B coefficients derived from the exponential fit accurately predict the minimum voltages (Table 2);
- Differences between numerical and analytical solutions of Stoletov's points are ≲2%;
- Mars minimum breakdown voltages are lower than Earth due to Martian atmospheric pressure (0.6% P_{Earth}).

Coefficients	Raizer (1991)	Bolsig+ (Earth)	Morrow and Lowke (1997)	Bolsig+ (Mars)
A (1/cm/Torr)	15	9.29	7.7	33.44
B (V/cm/Torr)	365	295.18	274.7	430.07

Table 2: Exponential approximation coefficients (A and B) from figure 6 found from fitting: $\alpha_{eff}(E) = Ape^{\left(\frac{-Bp}{E}\right)}$

Stoletov's Point V_{min} (V)	Analytical	Numerical	Error (%)
Cartesian (Earth)	918.6	912.4	0.7%
Spherical (Earth)	1178.3	1136.1	3.7%
Cartesian (Mars)	358.9	356.1	0.8%
Spherical (Mars)	682.9	668.8	2.1%

Table 3: The minimum breakdown voltages for each geometry and atmosphere; also known as Stoletov's points $\frac{\partial V}{\partial R_1} = 0$.

IV. CONCLUSIONS

The results and conclusions obtained in this work can be summarized as follows:

- A new model for calculations of the critical radius and minimum breakdown voltage for Corona discharge in Cartesian and spherical geometries is presented;
- The model is validated using classic Paschen theory and experimental data in air from Meek and Craggs (1978);
- We expand classic Paschen theory into an analytical solution for spherical geometry;
- Our numerical model and the analytical solution show excellent agreement;
- The significantly lower pressure on Mars compared to Earth lowers the minimum breakdown voltage required to create discharge.

Acknowledgements:
This work is supported by the Embry-Riddle Aeronautical University (ERAU) and the Center for Space and Atmospheric Research (CSAR).

REFERENCES

- E. Berkoff, "The Corona Discharge: It's Properties and Uses- Colorado Wire & Cable (2015).
- W. M. Farrell and M. D. Desch. Is there a Martian atmospheric electric circuit? *J. Geophys. Res.*, 106:7591–7596, 4 2001. doi: 10.1029/2000JE001271.
- J. Gewartoski, J. W. Watson, H. Alexander. Principles of Electron Tubes: Including Grid-controlled Tubes, Microwave Tubes and Gas Tubes,' D. Van Nostrand Co., Inc. (1965).
- A. S. Gibson, J. A. Riousset, and V. P. Pasko. 'Minimum breakdown voltages for corona discharge in cylindrical and spherical geometries,' NSF EE REU Penn State Annual Research Journal, 7, 1-17 (2009).
- G. J. M. Hagelaar and L. C. Pitchford. Solving the Boltzmann equation to obtain electron transport coefficients and rate coefficients for fluid models. *Plasma Sources Sci. Technol.*, 14(4):722–733, 2005.
- W. A. Lyons, CCM, T. E. Nelson, R. A. Armstrong, V. P. Pasko, and M. A. Stanley. Upward electrical discharges from thunderstorm tops. *Bull. Am. Meteorol. Soc.*, 84(4):445–454, 2003. doi: 10.1175/BAMS-84-4-445.
- J. M. Meek and J. D. Craggs. *Electrical Breakdown of Gases*. John Wiley and Sons, New York, NY, 1978.
- C. B. Moore, W. Rison, J. Mathis and G. Aulich, 'Lightning rod improvement studies,' J. Appl. Meteor., 39 (5) 593- 609 (2000)
- R. Morrow and J. J. Lowke. Streamer propagation in air. *J. Phys. D: Appl. Phys.*, 30:614–627, 1997.
- Y. P. Raizer. *Gas Discharge Physics*. Springer-Verlag, New York, NY, 1991.
- R. Whetmore, 'Electrical Energy,' In Compton's by Brittanica (2016).
- Y. Yair. New results on planetary lightning. *Adv. Space Res.*, 50(3):293–310, 8 2012. doi: 10.1016/j.asr.2012.04.013.